Supporting Information

A Multifunctional Mo-N/Fe-N Interfaced MoS_2/FeNC Electrocatalyst for Energy Conversion Application

Khatun A Jannath,[†a] Kyubin Shim,[†b] Kyeong-Deok Seo,[†a] Heru Agung Saputra,[a] Sang Mun Lee,[b] Hae Jin Kim,[b] and Deog-Su Park*[a]*

[a] Department of Chemistry and Chemistry Institute for Functional Materials, Pusan National University, Busan, 46241, Republic of Korea

[b] Research Center for Materials Analysis, Korea Basic Science Institute, Daejeon 34133, Republic of Korea

[*] Corresponding authors: Dr. Hae Jin Kim Prof. Deog-Su Park

E-mail: hansol@kbsi.re.kr, dsupark@pusan.ac.kr

Tel.: +82-42-865-3953, +82-51-510-2244; Fax: +82-51-514-2122

[1] These authors contributed equally to this work.

Simulated Structures	Total Energy
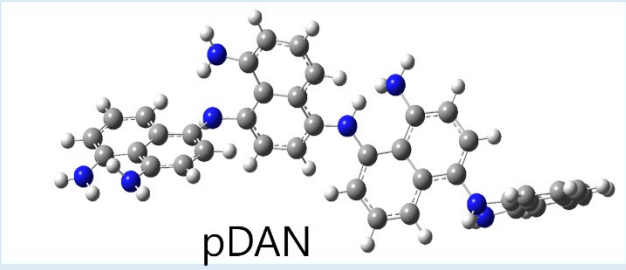 pDAN	-1982 a.u.
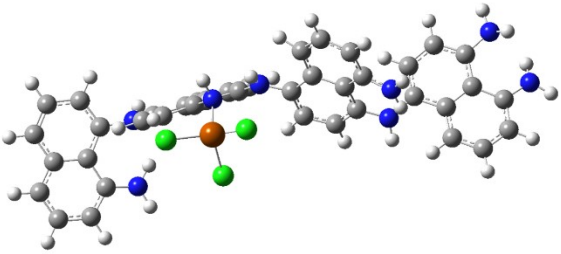 Fe-pDAN (**Fe coordination with one -NH_2**)	-2150 a.u.
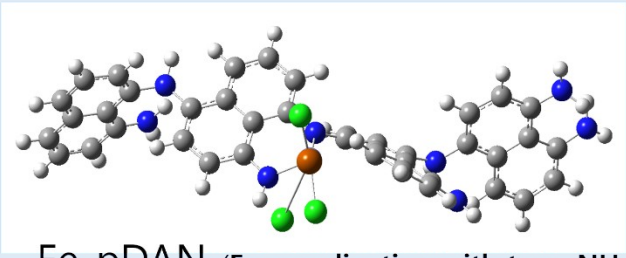 Fe-pDAN (**Fe coordination with two -NH_2**)	-2149 a.u.

Table S1: Simulated structures and the energy values for pDAN and Fe-pDAN.

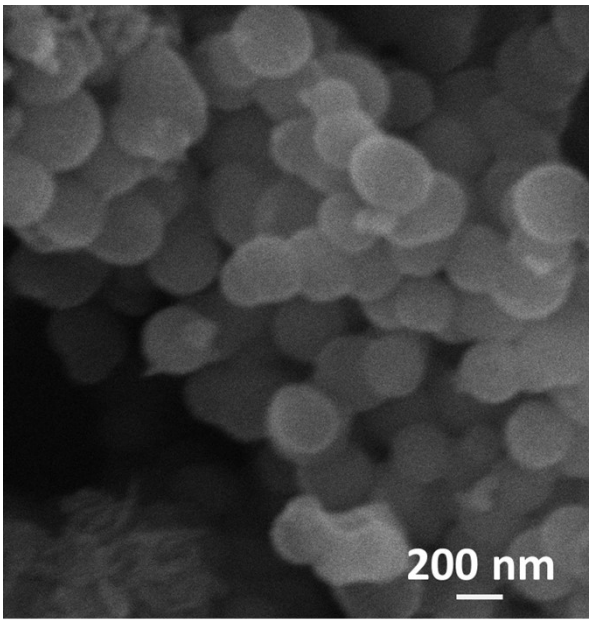

Figure S1: SEM image of FeNC.

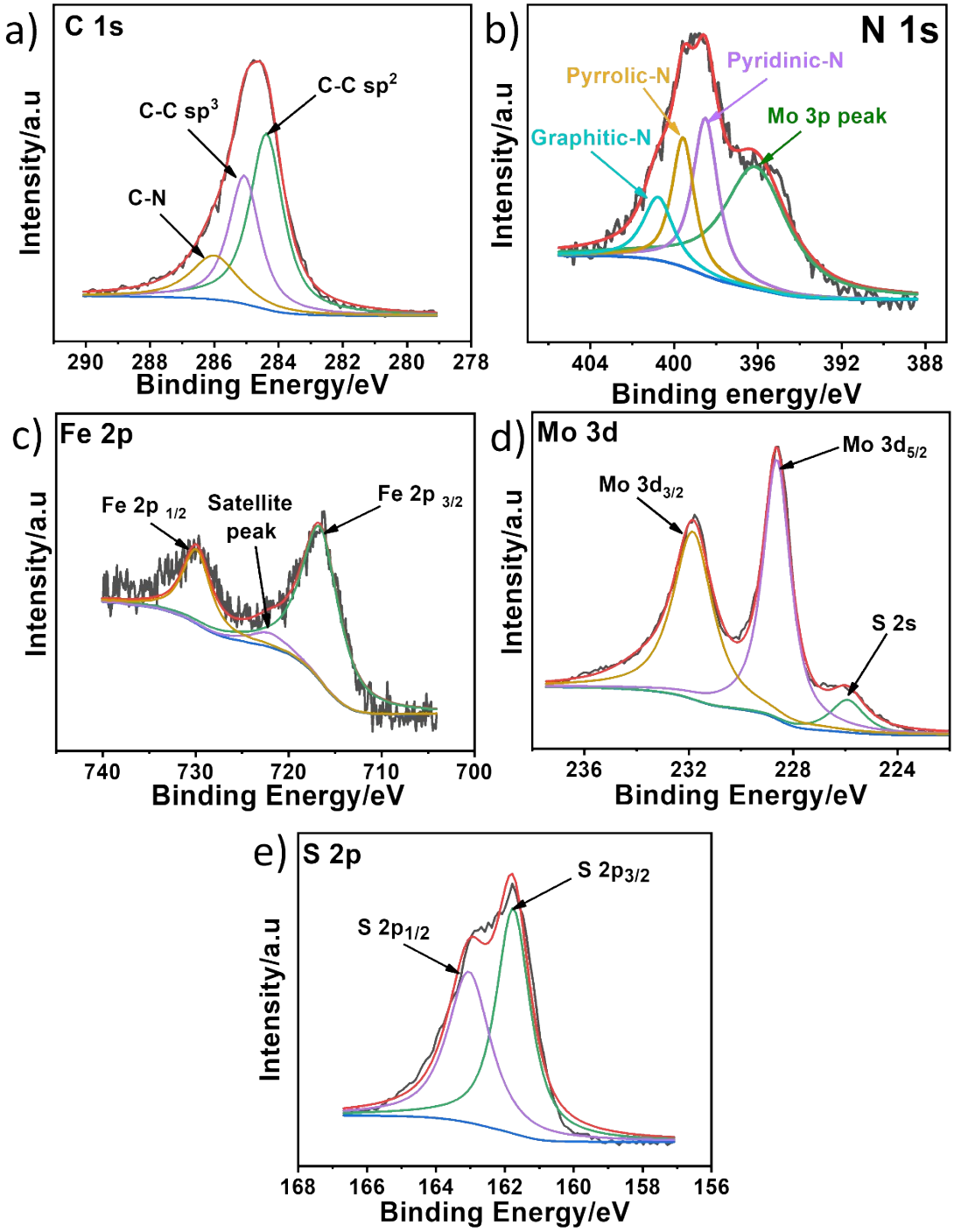

Figure S2: High-resolution XPS images of a) C 1s, b) N 1s, c) Fe 2p, d) Mo 3d, and e) S 2p for MoS_2@FeNC.

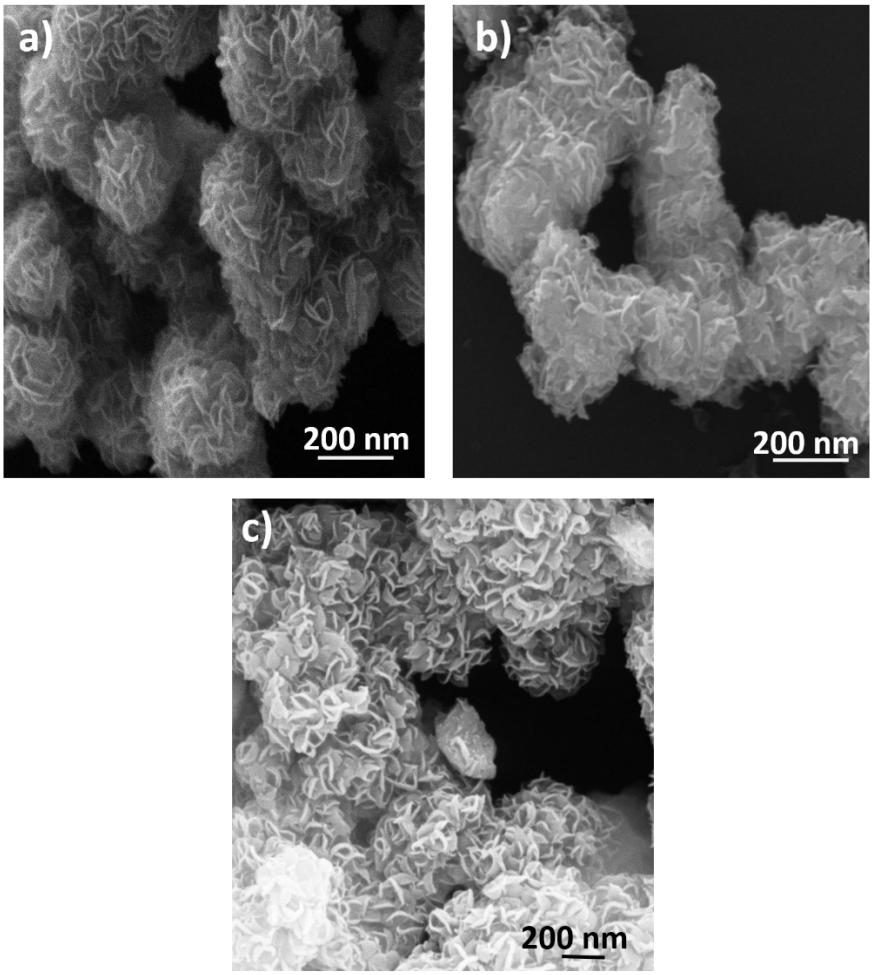

Figure S3: SEM images of a, b) MoS_2/FeNC pyrolyzed at 700 and 900 °C, respectively. SEM image of c) MoS_2-800.

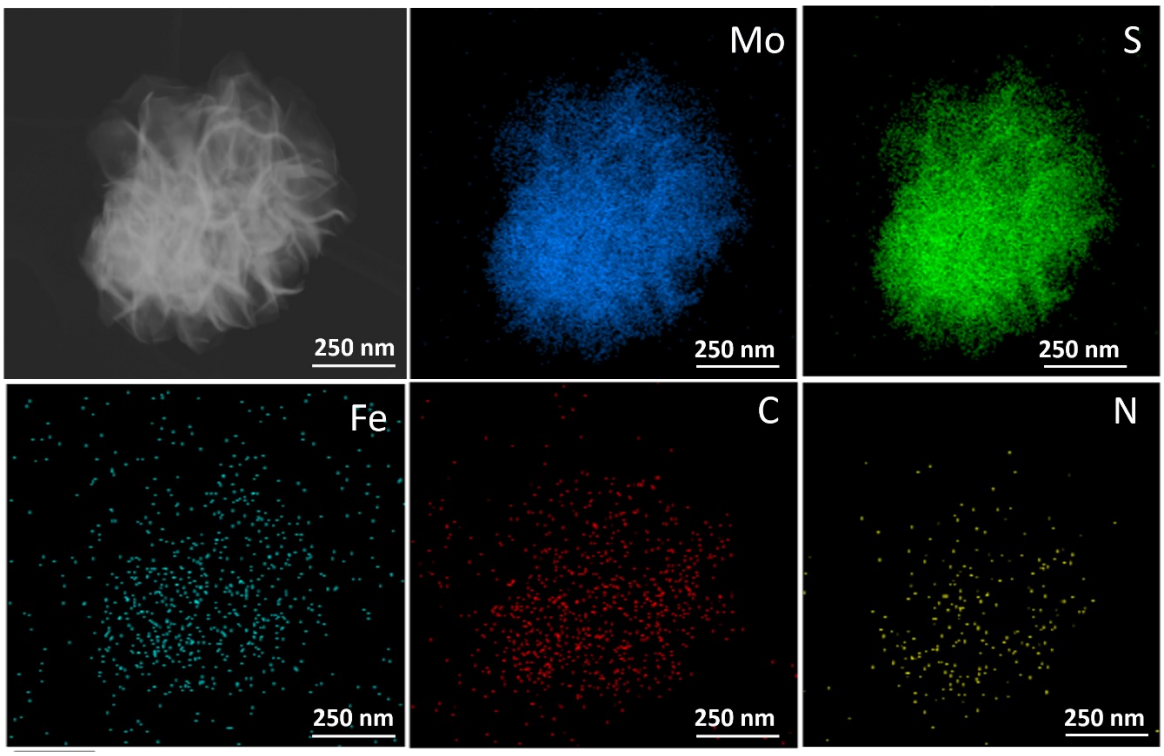

Figure S4: a) Dark-field TEM image of MoS_2/FeNC-800 and the corresponding elemental mapping images of Mo, S, Fe, C, and N.

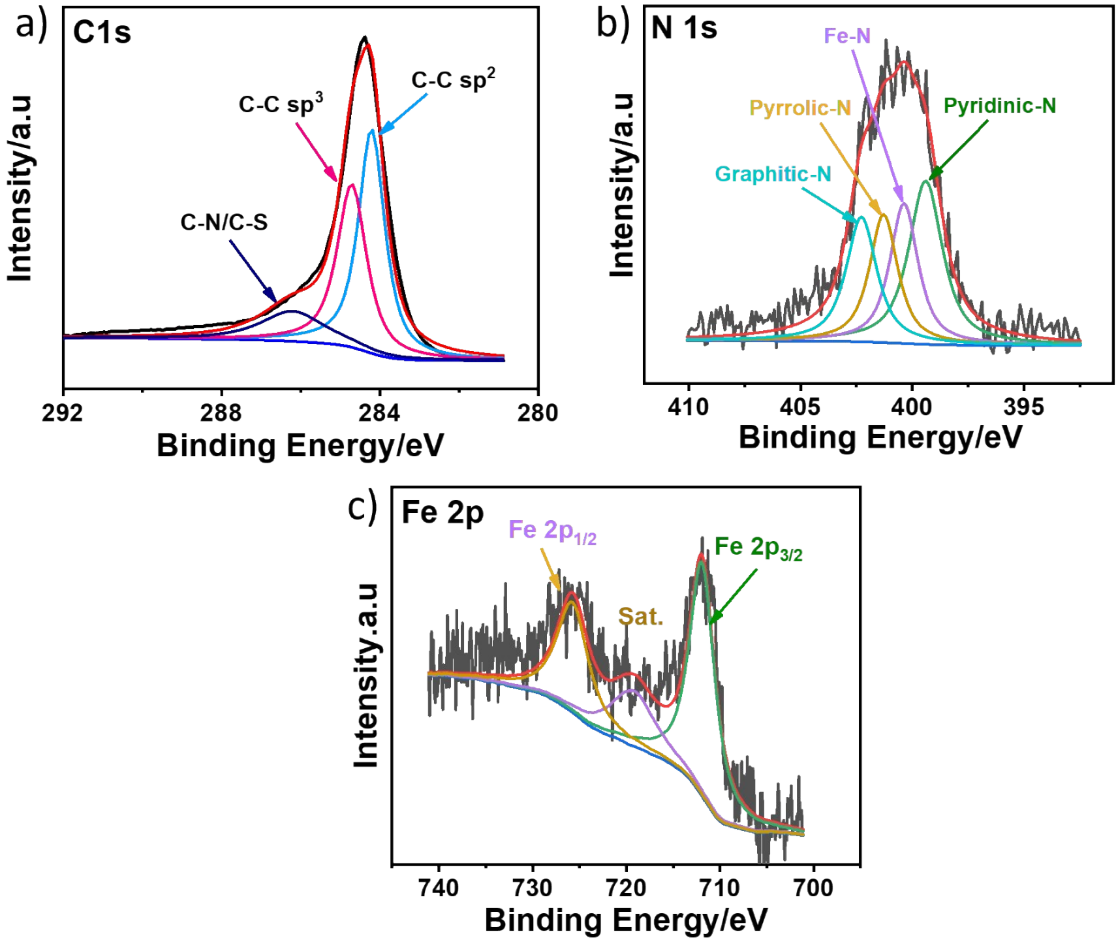

Figure S5: High-resolution XPS spectrum of a) C 1s, b) N 1s, and c) Fe 2p for FeNC-800.

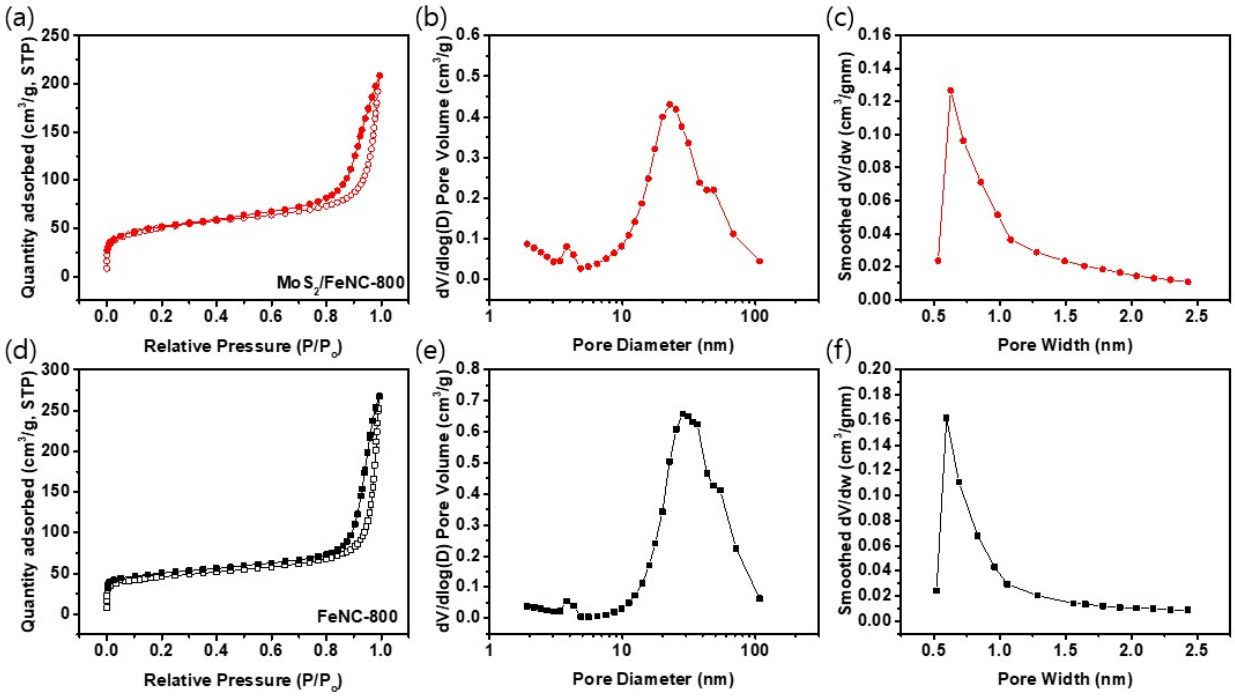

Figure S6: N_2-adsorption/desorption isotherms (a) MoS_2/FeNC-800 and (b) FeNC-800. Pore size distributions obtained by the BJH method for (b) MoS_2/FeNC-800 and (e) FeNC-800. Pore size distributions obtained by the HK method for (c) MoS_2/FeNC-800 and (f) FeNC-800

Table S2. The pore structure of the sample, as determined using BET method and t-plot.

Samples	S_{BET} (m^2/g)	S_{ext} (m^2/g)	V_{mic} (cm^3/g)	V_{tot} (cm^3/g)	D_{avg} (nm)	Avg. w_{HK} (nm)
FeNC	164.6	80.9	0.04	0.39	9.50	0.69
MoS_2/FeNC	180.2	104.5	0.03	0.32	7.17	0.80

S_{BET}: Specific surface area by BET plot

S_{ext} : External surface area by t-plot

V_{mic}: Micropore volume by t-plot (<2nm)

V_{tot}: Total pore volume

D_{avg}:. Average pore diameter(4V/A: by BET)

Avg. w_{HK} : Average pore diameter by H-K method(<2nm)

*** Notes on BET analysis.**

The typical sample weight was 50–100 mg. Before measurement, the sample was degassed under a vacuum of 1.33×10^{-6} kPa at 363 K for 1 hour, then it was heated at a rate of 5 K/min to 393 K overnight. The adsorption-desorption measurements were carried out at a liquid nitrogen temperature (77 K). The specific surface area (S_{BET}), the micropore volume (V_{mic}), and the external surface area were determined by means of a t-plot. The total pore volume (V_{tot}) was calculated at a relative pressure of $P/P_0 = 0.9889$. The pore sizes of the sample were analyzed using the Horvath-Kawazoe (H-K) method for microporosity and the Barrett-Joyner-Halenda (BJH) method for mesoporosity.

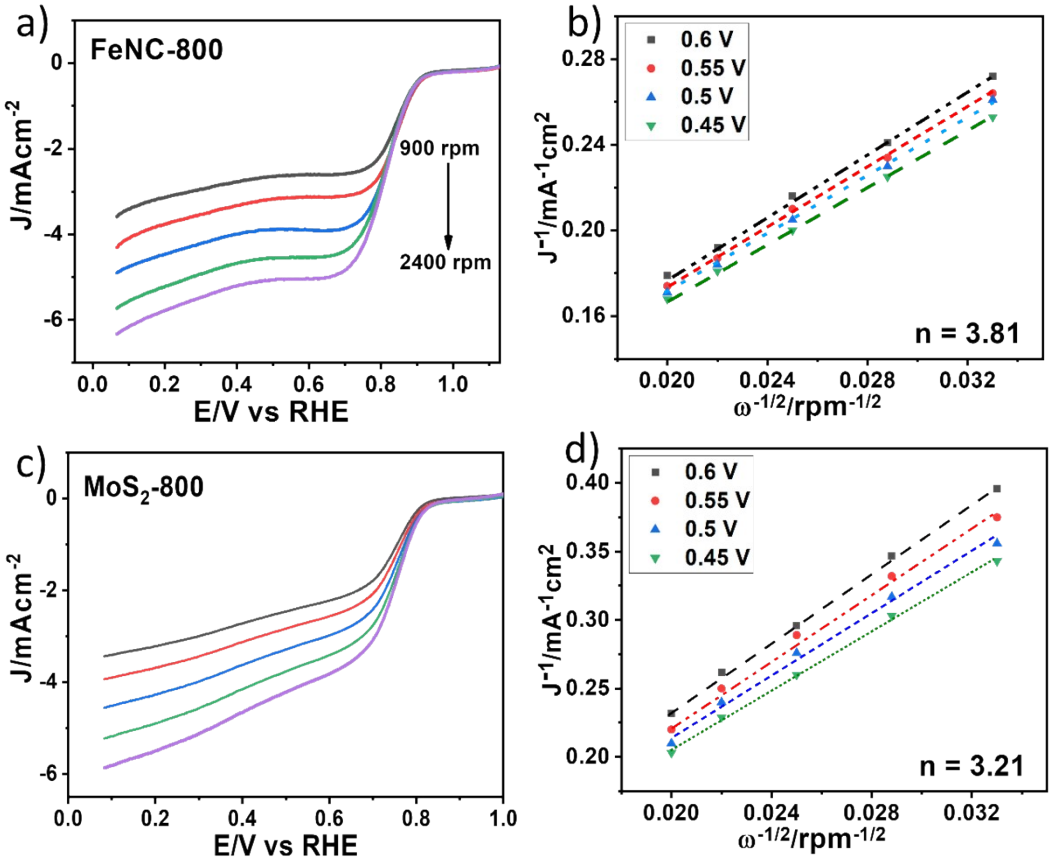

Figure S7: a) RDE polarization curves of FeNC-800 at different rotation rates, b) corresponding KL plot. c) RDE polarization curves of MoS_2-800 at different rotation rates, d) corresponding KL plot.

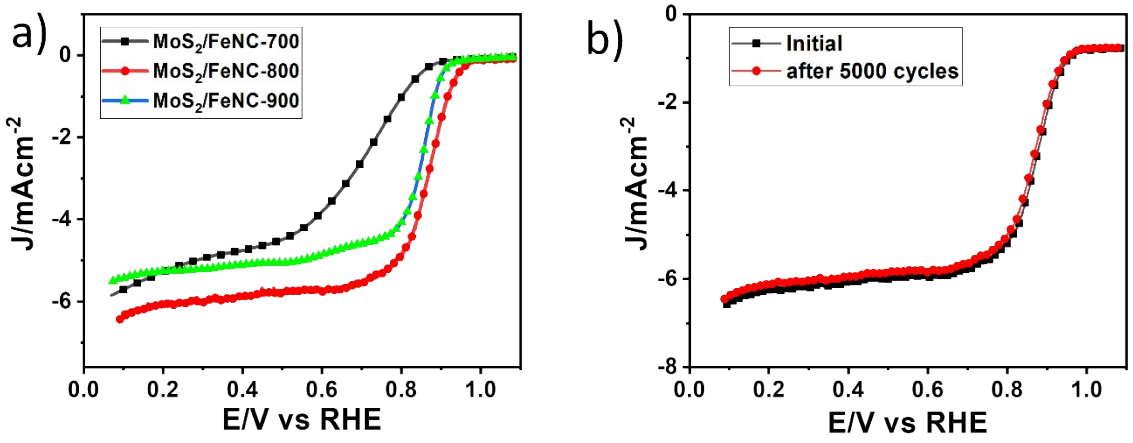

Figure S8: a) LSVs of MoS_2/FeNC prepared at different pyrolysis temperatures for ORR in 0.1 M KOH. b) Stability of MoS_2/FeNC-800 after 5000 cycles.

Table S3: Comparison of HER catalytic activities between MoS_2@FeNC and other well-developed HER electrocatalysts and non-noble metal catalysts in 1 M KOH.

Catalysts	**Overpotential (η) at 10 $mAcm^{-2}$**	**Tafel slope**	**Electrolyte**	**References**
MoS_2/FeNC-800	**128 mV**	**61 mV dec^{-1}**	**1 M KOH**	**This work**
Ni-1T MoS_2	199 mV	52.7 mV dec^{-1}	1 M KOH	Small, 2022, 18, 2107238
NiS@MoS_2	146 mV	62.44 mV dec^{-1}	1 M KOH	Journal of Alloys and Compounds, 2021, 853, 157352
MoS_2@$CoSe_2$-CC	101 mV	67 mV dec^{-1}	1 M KOH	Nanoscale, 2022, 14, 2490-2501
V doped MoS_2	206 mV	59 mV dec^{-1}	1 M KOH	Applied Catalysis B, 2019, 254, 432-442
CoS_2-MoS_2	130 mV	66.8 mV dec^{-1}	1 M KOH	Applied Surface Science, 2020, 527, 146847
NiS/MoS_2	174 mV	70.2 mV dec^{-1}	1 M KOH	J. Mater. Chem. A, 2019, 7, 21514-21522
Fe, C-MoS_2/Ni_3S_2-450	188 mV	95 mV dec^{-1}	1 M KOH	Crystals, 2021, 11, 340
Co_3O_4@MoS_2/CC	207 mV	59.5 mV dec^{-1}	1 M KOH	J. Mater. Chem. A, 2018, 6, 2067-2072

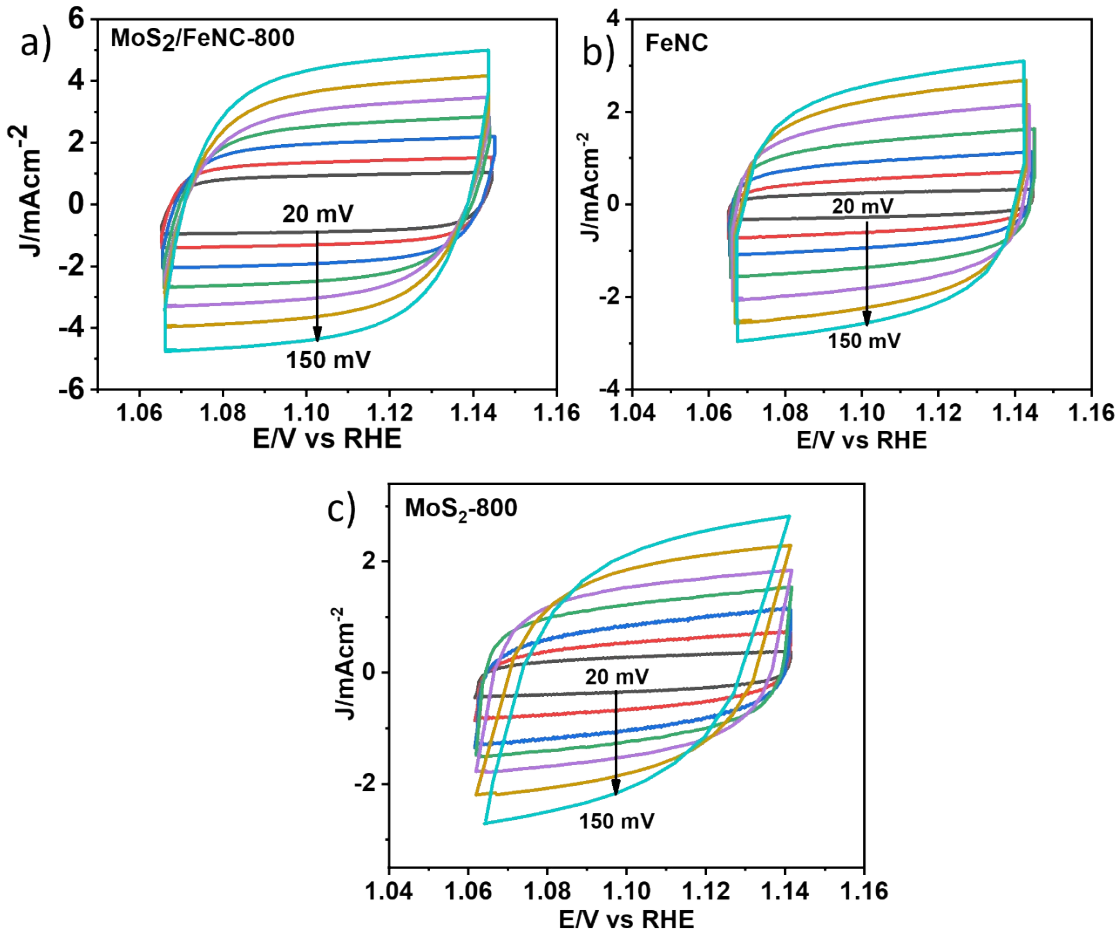

Figure S9: CV curves MoS_2/FeNC-800, FeNC-800, and MoS_2 -800 at different scan rates.

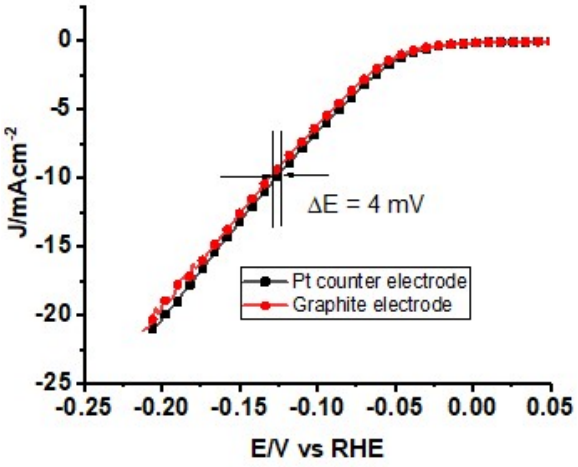

Figure S10: Comparison of LSVs of MoS_2/FeNC-800 using graphite rod (red line) and platinum wire (black line) as the counter electrode.

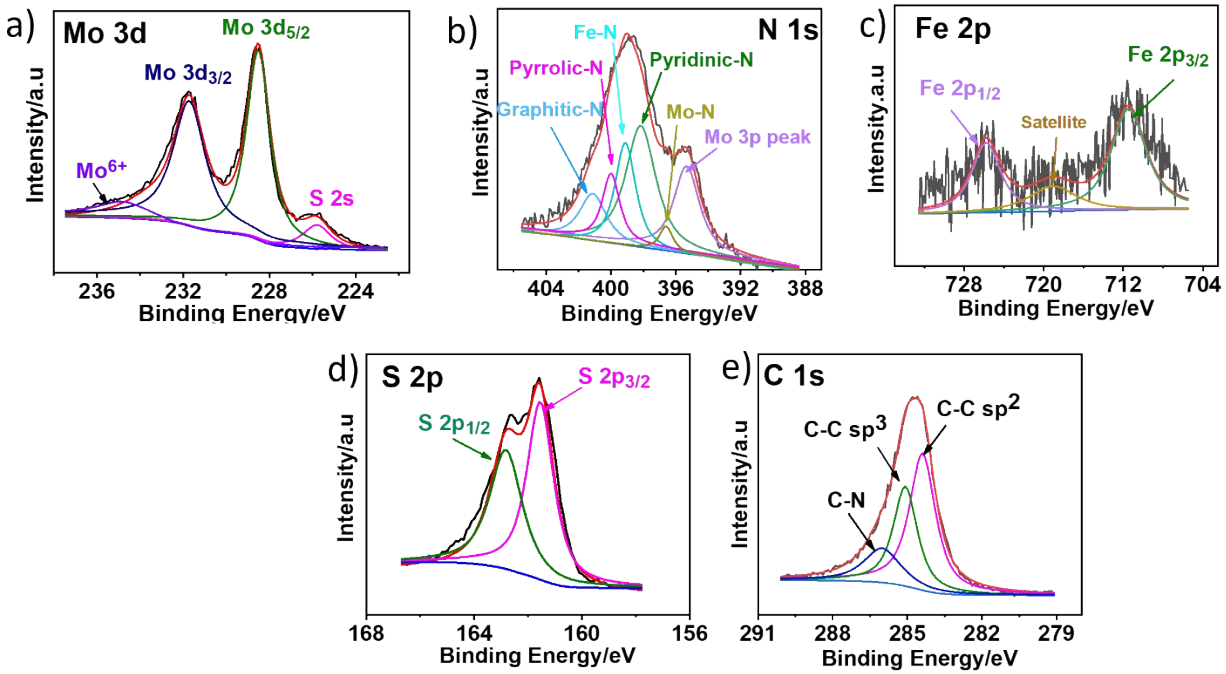

Figure S11: High-resolution XPS spectra of a) Mo 3d, b) N 1s, c) Fe 2p, d) S 2p, and e) C 1s for MoS_2/FeNC-800 after long-term chronoamperometric study.

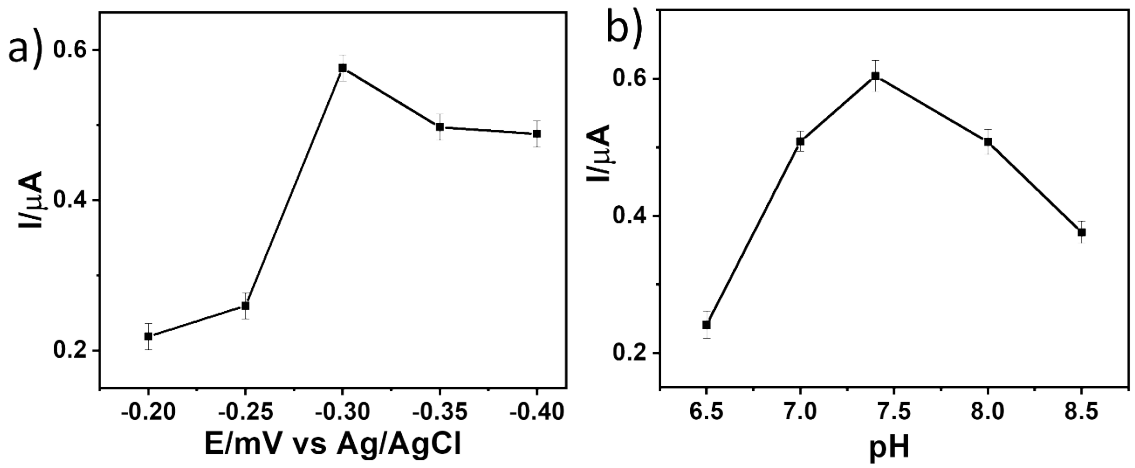

Figure S12: Optimization of a) potential, b) pH for H_2O_2 sensor measurements in PBS (pH 7.4).